Mohammed Rafi Shaik, Manawwer Alam* and Naser M. Alandis

Development of sustainable resource based poly(urethane-etheramide)/Fe_2O_3 nanocomposite as anticorrosive coating materials

Abstract: Linseed polyetheramide (LPEtA) resin was synthesized by the condensation polymerization of N-N-bis (2-hydroxyethyl) linseed oil fatty amide (HELA) with pyrogallol. The residual hydroxyl groups of LPEtA resin were further modified with isophorone diisocyanate (IPDI) to obtain linseed poly(urethane-etheramide) (ULPEtA) via addition polymerization. ULPEtA was modified with iron oxide nanoparticles in different weight percent (0.1 wt%, 0.2 wt%, 0.3 wt% and 0.4 wt%) producing ULPEtA/Fe_2O_3 nanocomposite. Spectroscopic characterization of HELA, LPEtA and ULPEtA was carried out by using Fourier transform infrared (FT-IR), proton nuclear magnetic resonance (^{1}H-NMR) and carbon nuclear magnetic resonance (^{13}C-NMR) techniques. Physicochemical and physico-mechanical properties of LPEtA and ULPEtA were carried out by using standard methods. Thermal stability and anticorrosion performance were assessed by thermogravimetric analysis/differential scanning calorimetry (TGA/DSC) and potentiodynamic polarization. The corrosion behavior of ULPEtA/Fe_2O_3 nanocomposite coatings on mild steel was investigated in different corrosive environments (3.5 wt% HCl, 5.0 wt% NaCl, 3.5 wt% NaOH, and tap water) at room temperature. Surface morphology study was performed through scanning electron microscopy (SEM) and energy dispersive X-ray (EDX). Coating properties such as gloss, scratch hardness, flexibility and impact resistance were evaluated using standard methods. The results of this study showed that ULPEtA/Fe_2O_3 nanocomposite coatings exhibit good physico-mechanical, anticorrosive properties and can be safely used up to 220°C.

Keywords: anticorrosive coatings; linseed oil; poly(urethane-etheramide); pyrogallol.

***Corresponding author: Manawwer Alam,** Research Center, College of Science, King Saud University, P. O. Box 2455, Riyadh 11451, Saudi Arabia, e-mail: malamiitd@gmail.com
Mohammed Rafi Shaik and Naser M. Alandis: Department of Chemistry, College of Science, King Saud University, P. O. Box 2455, Riyadh 11451, Saudi Arabia

DOI 10.1515/polyeng-2015-0009
Received January 10, 2015; accepted March 2, 2015

1 Introduction

Corrosion of metallic structures is estimated to cost many billions of dollars annually. It is important to recognize that metallic corrosion under wet conditions involves oxidation and reduction reactions. The most common and efficient way to protect metallic substrates from corrosion involves application of organic coatings. These organic coatings protect the metals by formation of a barrier against oxygen and water [1–3].

Organic coatings are developed by various types of vegetable oils such as linseed, castor, soya bean, rapeseed, olive, cottonseed, jatropha, *Pongamia glabra*, rubber seed and others [4–8]. Vegetable oils are renewable, cost-effective, ecofriendly, abundantly available, nontoxic and biodegradable raw materials found in nature, having functional groups such as esters, carboxyls, active methylenes, double bonds and hydroxyls producing polyester, epoxies, alkyd, polyol, polyether, polyesteramide, polyetheramide, polyurethane and others. Vegetable oils have attracted massive consideration as potential sources of chemicals, at both laboratory and industrial scale for use in coatings, biodiesel, lubricants, folk medicines, cosmetics, plastics and paints [6, 9–14]. Vegetable oil based polyurethanes (PUs) occupy an important position due to their easy preparation methods, outstanding properties and versatile applications in coatings, foams, adhesives, sealants, elastomers and others [15–19].

In general, PUs are prepared by chemical reaction of a diol, polyol or polymer containing hydroxyl groups, with an aliphatic, cycloaliphatic or aromatic isocyanate such as isophorone diisocyanate (IPDI) [9], toluylene2,4-diisocyanate [11], 1,6-hexamethylenediisocyanate, cyclohexyldiisocyanate [16], 4,4'-diisocyanato dicyclohexylmethane [20] and 4,4'-methylenebis(phenyl isocyanate) [21, 22]. Vegetable oil based PU films have shown good toughness, scratch resistance and impact resistance in coatings and

paints. The properties of PUs obtained from vegetable oil derivatives depend on a number of factors such as fatty acid composition, number of hydroxyl groups and structures of isocyanates [16].

Fe_2O_3 possess magnetic, electric and corrosion inhibition properties. These have attracted considerable attention for their application as fillers/pigments in polymeric coating materials [23–26]. These protect the degradation by sunlight, acid, alkali and moisture. They have nonbleeding and nonfading pigment properties and nanosized particles also improve the physico-mechanical and thermal properties, relative to conventional Fe_2O_3 particles [24].

In the present work, chemical modification of linseed oil based N-N-bis (2-hydroxyethyl) fatty amide (HELA) was carried out with pyrogallol to obtain linseed polyetheramide (LPEtA). LPEtA was treated with IPDI at a certain temperature to synthesize linseed poly(urethane-etheramide) (ULPEtA) which was reinforced with Fe_2O_3 nanoparticles to form poly(urethane-etheramide)/Fe_2O_3 nanocomposite coatings. LPEtA and ULPEtA were characterized using Fourier transform infrared (FT-IR), proton nuclear magnetic resonance (^{1}H-NMR) and carbon nuclear magnetic resonance (^{13}C-NMR) spectroscopic techniques. The incorporation of ether and urethane moieties in polymer chains is expected to improve its physico-mechanical and chemical resistance performance.

2 Materials and methods

2.1 Materials

Linseed oil, (WinLab, Middlesex, UK) with fatty acid composition (linolenic acid 44%, linoleic acid 14% and oleic acid 20%) [27], sodium, methanol, ethyl acetate (Sigma Aldrich, Steinheim, Germany), diethanolamine (Winlab, Leicestershire, UK), pyrogallol (E Merck, Darmstadt, Germany), Iron oxide (size 28–32nm, Sigma-Aldrich, Steinheim, Germany), Xylene (WinLab, Middlesex, UK) and IPDI (ACROS Organics, New Jersey, USA) were of analytical grade.

2.2 Characterization

HELA, linseed oil polyetheramide (LPEA) and linseed oil poly(urethane-etheramide) resins were characterized by FT-IR, ^{1}H-NMR and ^{13}C-NMR spectroscopic techniques. FT-IR spectra were produced using NaCl window by Pristige-21, FTIR-8400S, Shimadzu Corporation, Kyota, Japan in the range of 4000–400 cm^{-1}. ^{1}H-NMR and ^{13}C-NMR spectra were recorded on JEOL DPX 400 MHz using deuterated chloroform as solvent and tetramethylsilane as internal standard. Thermogravimetric analysis (TGA) and differential scanning calorimetry (DSC) were carried out by TGA/DSC1 Mettler Toledo AG, Analytical CH-8603, Schwerzenbach, Switzerland. In TGA, an approximately 6 mg sample (ULPEtA40/Fe_2O_3) was loaded in an alumina crucible and heating was accomplished from 25°C to 600°C at 10°C/min in nitrogen atmosphere with flow 20 ml/min. In DSC, about 5 mg of ULPEtA40/Fe_2O_3 was loaded in aluminum pan and heating was carried out from 25°C to 400°C at 10°C/min in nitrogen atmosphere with flow 20 ml/min. TGA and DSC both were previously calibrated by standard indium. Morphological observations of ULPEtA40/Fe_2O_3 were made by scanning electron microscopy (SEM) (Jeol, JED-2200 series, Japan). For SEM-energy dispersive X-ray (EDX) observations, the coating was uniformly spread on a carbon tape and coated with a thin conducting layer of platinum (Pt). The morphological properties of samples were examined at room temperature and with a spectrometer for EDX analysis sapphire with an ultra-thin window. The surface of the detector is 10 mm^2. Acid value (ASTM D55-61), hydroxyl value (ASTM D1957-86), iodine value (ASTM D1959-97) and refractive index (ASTM D1747-09) were measured by Abbe's refractometer. The reaction was monitored by thin layer chromatography (TLC) taken at regular intervals of time at room temperature. TLC was taken on a silica gel coated aluminum sheet (stationary phase) and ethyl acetate (mobile phase). First, one spot of each resin like HELA, pyrogallol and LPEtA (well diluted with known dilution) was put on the TLC plate, 1 cm from the base, at regular distances between them. The spots were then dried. The spotted TLC sheet was then kept in ethyl acetate solvent in the developer tank, keeping the solvent level below the spot. When the sample had moved upwards on the TLC plate to the desired distance, the TLC plate was taken out of the tank, dried again and placed in an iodine chamber for visualization.

2.3 Synthesis of HELA

HELA was prepared according to a previously reported method [27].

2.4 Synthesis of LPEA

Amounts of 5.74 g of HELA, 1.26 g of pyrogallol and 0.2 g of *p*-toluene sulfonic acid were dissolved in 70 ml of xylene

and placed in a three-neck round bottom flask equipped with a Dean stark trap, thermometer and stirrer. The reaction mixture was heated at 120°C, the progress of the reaction was monitored by TLC and hydroxyl value was determined. The synthesized resin was also subjected to FT-IR analysis.

2.5 Synthesis of linseed oil poly(urethane-etheramide)

LPEtA was mixed with IPDI in different weight percent (30 wt%, 35 wt%, 40 wt% and 45 wt%) in xylene with continuous stirring in a three-neck flask under N_2 atmosphere at 160°C. The reaction was monitored by TLC as well as hydroxyl value determination. The synthesized resin was also subjected to FT-IR analysis.

2.6 Synthesis of linseed oil poly(urethane-etheramide)/Fe_2O_3 nanocomposites

Fe_2O_3 nanoparticles were added in the prepared ULPEtA in various concentrations, namely 0.1 wt%, 0.2 wt%, 0.3 wt%, and 0.4 wt%. The dispersion was carried out mechanically using a stirrer with a speed of 200 rpm for 30 min at room temperature. The 0.3 wt% nanoparticles showed the best dispersion in the polymer matrix.

3 Results and discussion

Steps 1 and 2 (Scheme 1) shows the synthesis of LPEtA, and ULPEtA, respectively. Synthesis of LPEtA was carried out from the reaction of HELA with pyrogallol and further treated with IPDI to form ULPEtA. The addition of Fe_2O_3 nanoparticles to ULPEtA resulted in ULPEtA/Fe_2O_3 nanocomposites. The structural features of HELA, LPEtA and ULPEtA were confirmed by FT-IR, ^{1}H-NMR and ^{13}C-NMR spectral analysis.

3.1 Spectral analysis

3.1.1 FT-IR

FT-IR spectra of HELA showed the characteristic bands at 1650 cm^{-1} for CO amide, 3368 cm^{-1} for hydroxyl group, and 2854 cm^{-1} and 2926 cm^{-1} for symmetrical and asymmetrical stretching, respectively. The bands at 1467 cm^{-1} appear for C-N stretching and 3010 cm^{-1} for unsaturation of the alkyl chain. LPEtA showed some additional characteristic bands at 1207 cm^{-1} for alkyl aryl ether, 3368 cm^{-1} for terminal hydroxyl group, and at 3009 cm^{-1}, 771 cm^{-1} and 720 cm^{-1} for aromatic ring of pyrogallol. LPEtA was treated with IPDI to form urethane linkages. ULPEtA shows some additional bands at 1715 cm^{-1} related to carbonyl of urethane and bands at 3323 cm^{-1} and 2270 cm^{-1} due to residual hydroxyl and isocyanate groups, respectively.

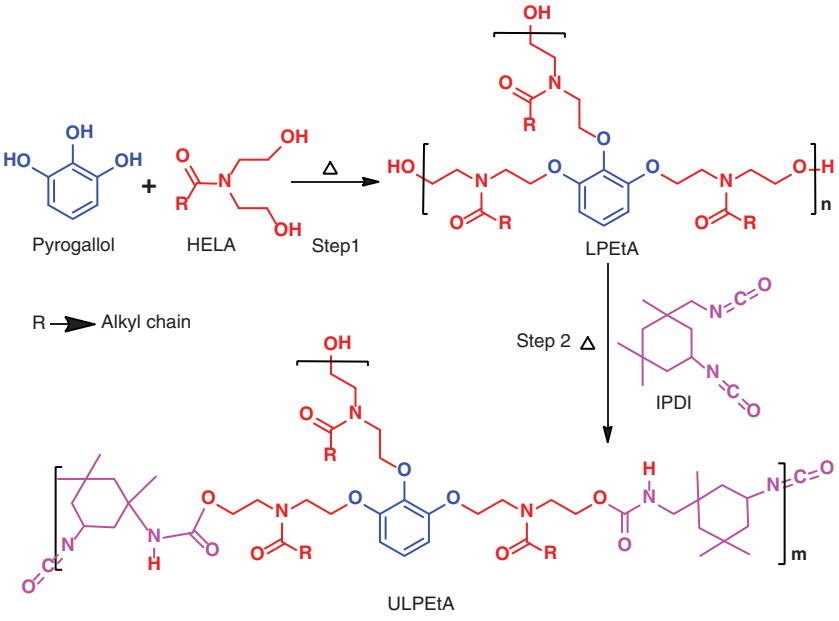

Scheme 1: Synthesis of linseed poly(urethane-etheramide) (ULPEtA).

3.1.2 ^{1}H-NMR

In ^{1}H-NMR spectra of HELA (Figure 1), terminal -C**H**$_3$ appeared at 0.88–0.98 ppm, the OH group is shown at 4.76 ppm, the peak at 3.49 ppm for -C**H**$_2$- attached to the hydroxyl group, the peak at 5.34 ppm for olefinic hydrogen, the peak at 1.26–1.30 ppm for internal -C**H**$_2$- of alkyl chain, the peak at 3.72 ppm for -C**H**$_2$- attached to amide nitrogen, the peak at 2.05–2.06 ppm for -C**H**$_2$- attached to unsaturation, and 2.77–2.79 ppm for -C**H**$_2$- attached between olefinic bonds. LPEtA (Figure 2) spectra showed some additional peaks at 4.17 ppm for -C**H**$_2$-O-aromatic ring, and peaks at 6.37–6.51 ppm for aromatic ring. In ULPEtA (Figure 3) along with some additional characteristic peaks at 8.01 for N**H** of urethane, the peak for -C**H**$_2$- attached to urethane linkage appeared at 2.58 ppm, those for -C**H**$_3$- of IPDI appeared at 0.97 ppm and those for the cyclic ring of IPDI occurred at 1.55 ppm. The residual -O**H** groups appeared at 5.40 ppm. These peaks supported the formation of urethane linkages.

3.1.3 ^{13}C-NMR

^{13}C-NMR spectra (Figure 4) of HELA revealed peaks at 14 ppm for terminal -**C**H$_3$, peak at 20–25 ppm for internal -**C**H$_2$-, peak at 26–28 ppm for -**C**H$_2$- attached to double bond, peak at 31–33 ppm for **C**H$_2$ attached to amide carbonyl, peak at 127–131 ppm for carbon of double bond, peak at 175 for amide carbonyl, peak at 58–63 ppm for -**C**H$_2$- attached to hydroxyl group and peak at 50–51 pm for -**C**H$_2$- attached to nitrogen. In the LPEtA spectrum (Figure 5), some

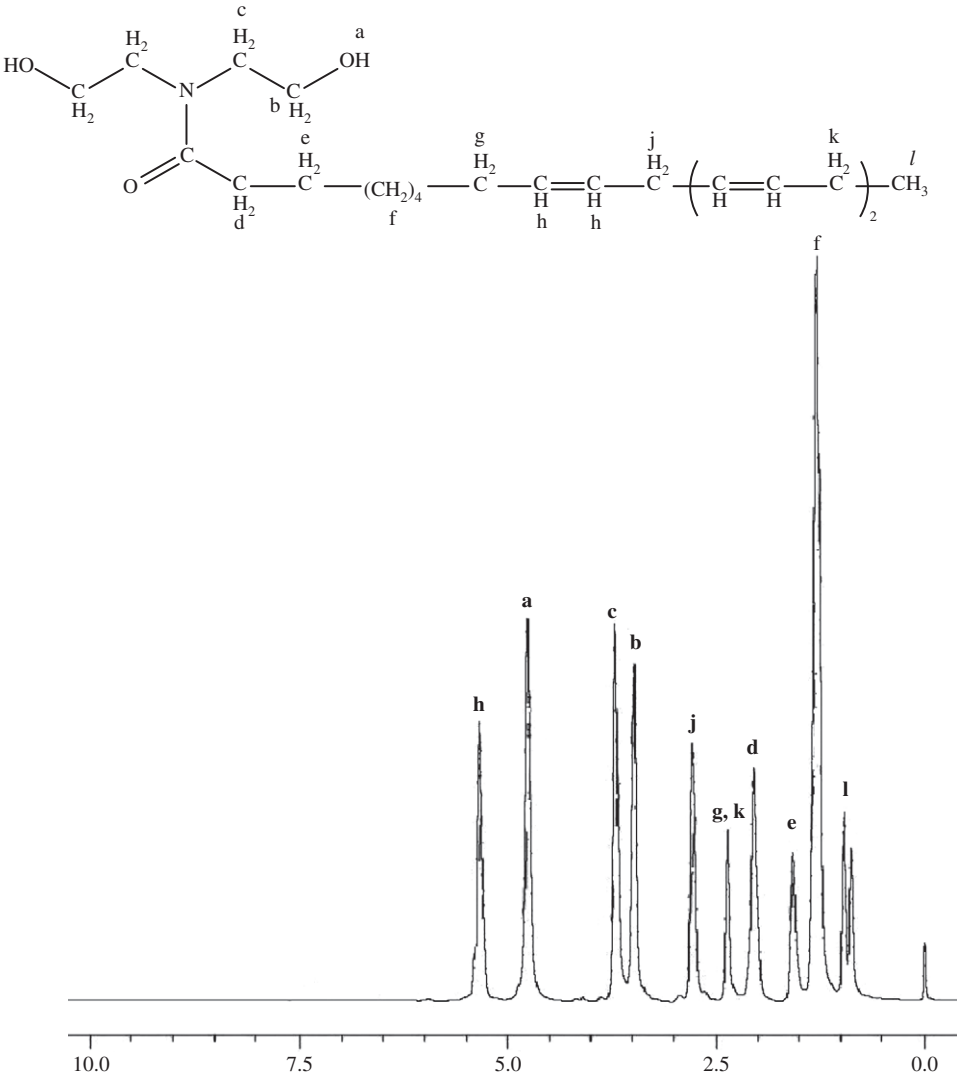

Figure 1: Proton nuclear magnetic resonance (^{1}H-NMR) spectra of N-N-bis (2-hydroxyethyl) linseed oil fatty amide (HELA).

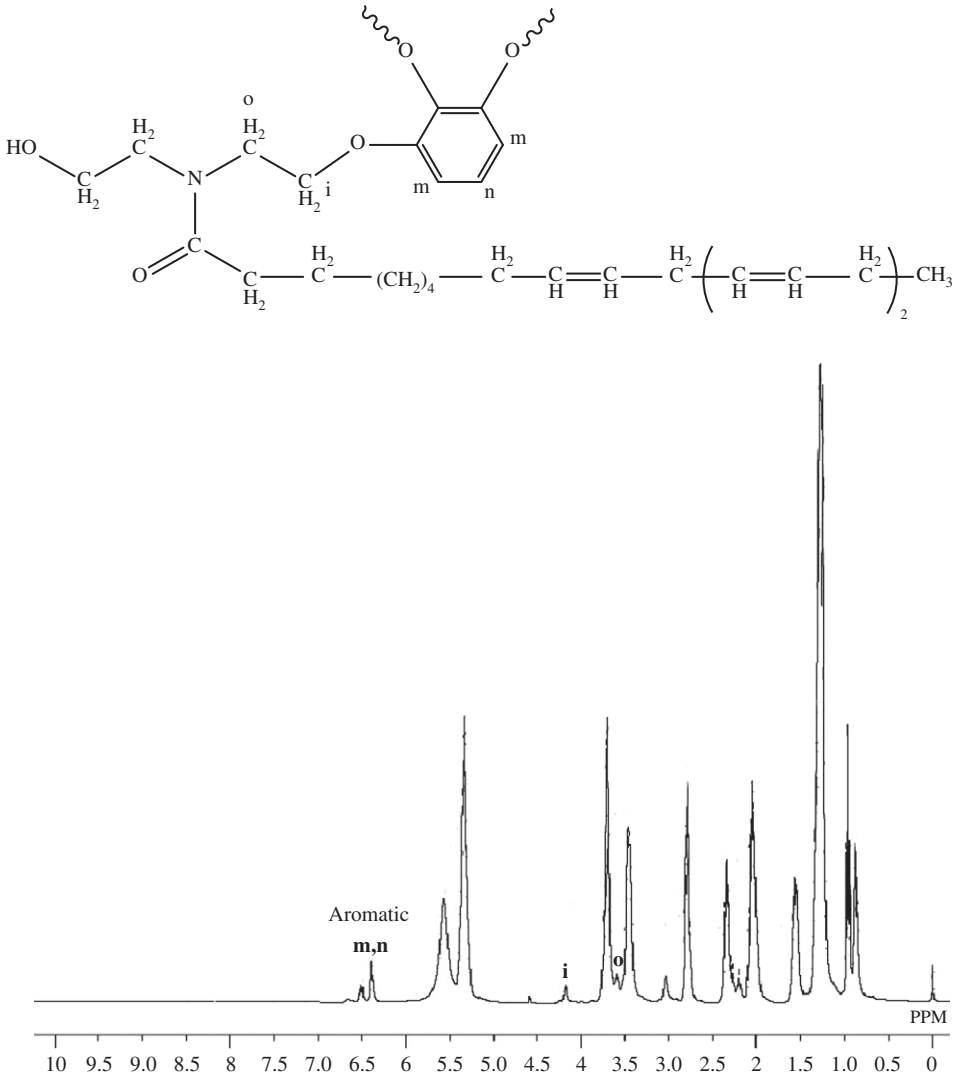

Figure 2: Proton nuclear magnetic resonance (^{1}H-NMR) spectra of linseed polyetheramide (LPEtA).

additional peaks appeared at 65 ppm for CH_2 attached to -O- for ether linkage, peak at 47 ppm for -**C**H_2- attached to nitrogen, and peaks at 107 ppm,118 ppm and 148 ppm for aromatic ring. In ULPEtA spectra (Figure 6) characteristic peaks appeared at 163 ppm for carbonyl of urethane, peak at 157 ppm for carbonyl of N**C**O group, peak at 19 ppm for **C**H_3 of IPDI, and peaks at 25 ppm, 23 ppm, 34 ppm and 35 ppm for cyclic ring.

3.2 Thermal analysis

The DSC thermogram (Figure 7) of ULPEtA40 nanocomposite showed endotherms starting at 72°C–192°C, centered at 147°C. This endothermic peak may be correlated to the melting phenomenon. The TGA thermogram of ULPEtA40 nanocomposite reveals 5% weight loss at 261°C, 20% weight loss at 346°C and 50% weight loss at 449°C. The degradation occurred in two steps; first step degradation for urethane linkages and second step degradation due to aromatic and aliphatic hydrocarbons. The inclusion of Fe_2O_3 in the matrix increased the thermal stability of the nanocomposite compared to plain resin (without nanoparticle), attributed to the interaction between the polymer matrix and large surface area of Fe_3O_4 nanoparticles, forming the stable nanocomposite [24, 27].

3.3 Preparation of coatings

A 40 wt% solution of ULPEtA nanocomposite resins was applied by dip technique on commercially available mild

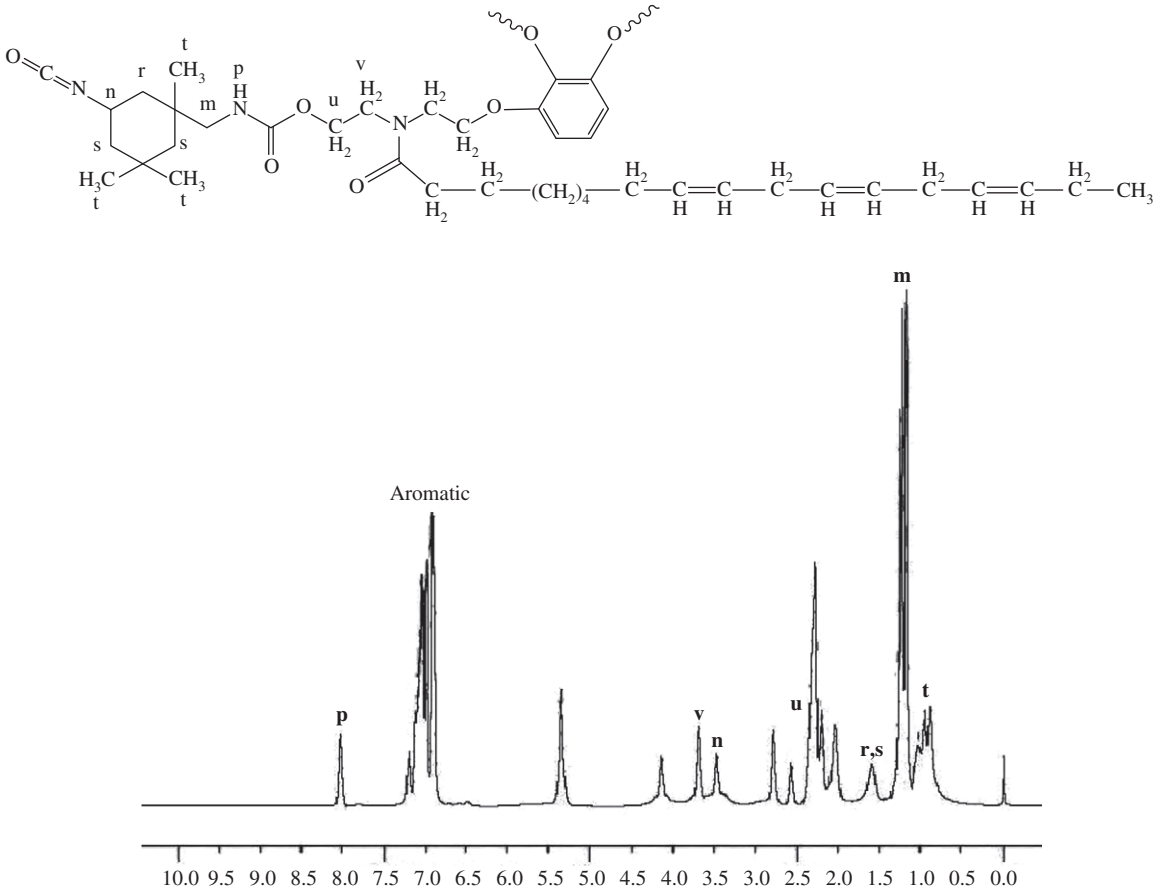

Figure 3: Proton nuclear magnetic resonance (^{1}H-NMR) spectra of linseed poly(urethane-etheramide) (ULPEtA).

steel strips with standard size (70 mm×25 mm×1 mm) for investigation. ULPEtA nanocomposite coatings on mild steel strips were tested for impact resistance (IS: 101 part 5/sec 3, 1988), scratch hardness (BS 3900), and bend test (1/8 inch conical mandrel, ASTM-D3281-84) performed on all compositions of ULPEtA coatings. Moreover, specular gloss of coatings was determined at 45°C using a gloss meter (Model RSPT 20; digital instrument, Santa Barba, CA, USA). Coating thickness was found to be 125–135 μm using the Elcometer (Model 345; Elcometer Instruments, Manchester, UK). Pencil hardness was assessed by a Wolff-Wilborn tester (Sheen Instruments, England). Corrosion resistance studies of ULPEtA-coated mild steel panels were performed using Gill AC (ACM Instruments, UK). A geometric area of 1 cm^2 each for coated mild steel was exposed to different corrosive media (3.5 wt% NaOH, 3.5 wt% HCl, 5 wt% NaCl and tap water). A Tafel curve was drawn using computer-controlled ACM Instruments provided with software. Corrosion current (I_{corr}) and corrosion potential (E_{corr}) were measured using potentiodynamic polarization. The corrosion inhibition efficiency was calculated according to our previously reported paper [13].

3.4 Physicochemical analysis

Table 1 showed that hydroxyl and iodine values decreased from HELA, LPEtA and subsequently to ULPEtA30, ULPEtA35, ULPEtA40 and ULPEtA45. The following trend may be correlated to the reaction of HELA with pyrogallol to form LPEtA, ensuing an increase in molecular weight, with increase in the amount of IPDI.

3.5 Physico-mechanical properties of coating

The coatings were dried at room temperature and drying times of these coatings were found to be about 15 min. According to results from Table 1, it can be seen that scratch hardness values were found to increase up to ULPEtA40 and after that a decrease in scratch hardness was observed. It is likely that additional NCO groups as functional sites render too much cross linking. All of the coatings passed the 150 lb/inch impact test, which showed a good interaction between metal substrate and organic coatings due to the presence of polar groups such as

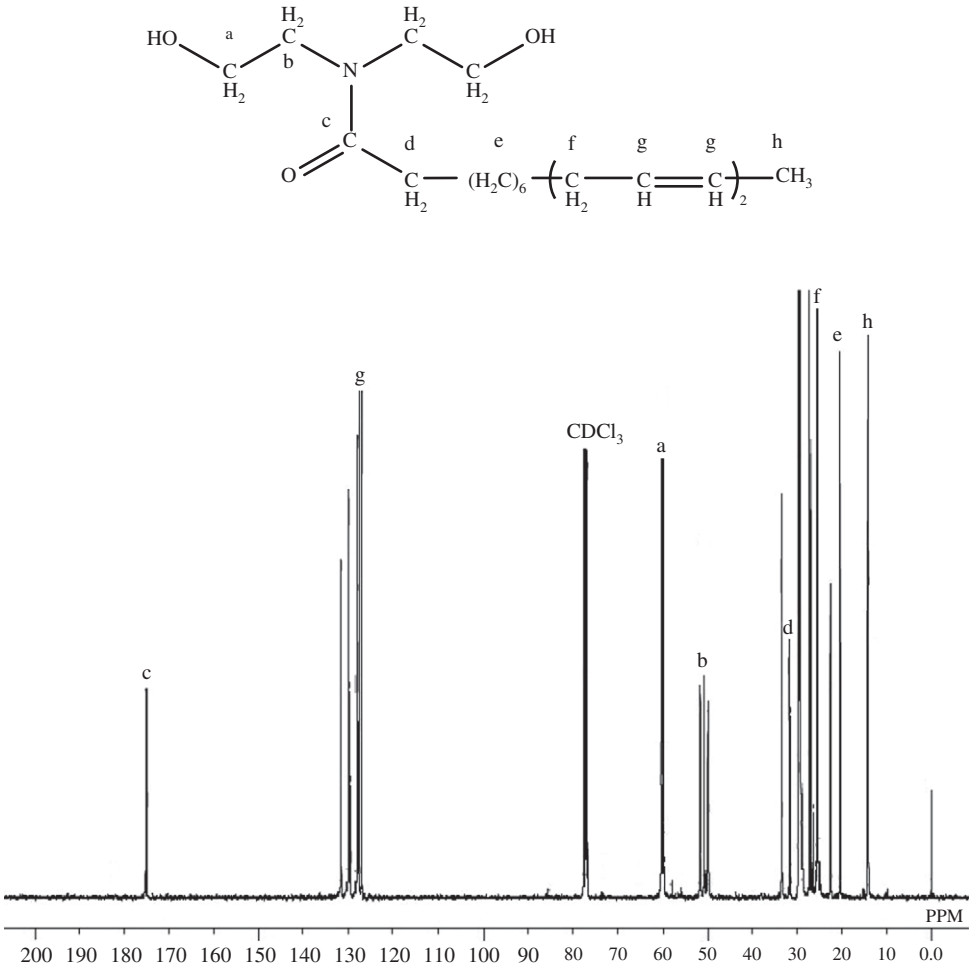

Figure 4: Carbon nuclear magnetic resonance (^{13}C-NMR) spectra of N-N-bis (2-hydroxyethyl) linseed oil fatty amide (HELA).

carbonyl, hydroxyl and urethane groups present in the polymeric chain. The coatings passed the bend test 1/8 inch conical mandrel, due to the presence of alkyl chains of oil. The coatings showed gloss values between 94 and 97 at 45° and passed the pencil hardness test maximum 6H showing good binding between the substrate and polymer coating.

3.6 Corrosion tests

The exposure of panels to 3.5 wt% HCl solution, 5 wt% NaCl solution, tap water and 3.5 wt% NaOH was carried out for 290 h, 175 h, 250 h and 2 h, respectively. The polarization curves in HCl solution for uncoated MS and coated with ULPEtA nanocomposites are shown in Figure 8. It was observed that there was a significant decrease for both anodic and cathodic currents of ULPEtA coating relative to uncoated MS. Anodic and cathodic current rates decreased, which can be described by the decrease in the active area of electrodes. The tabulated values of E_{corr}, I_{corr}, corrosion rate, and inhibition efficiency after 290 h of exposure in 3.5 wt% HCl solution are shown in Table 2. The results indicate a decrease in corrosion current of ULPEtA30, ULPEtA35, ULPEtA40 and ULPEtA45 nanocomposites as compared to uncoated mild steel. The $E_{corr,}$ corrosion rate for uncoated mild steel was -549.46 mV, 22.262 mm/year. The corrosion rate was controlled to lesser values (3.341×10^{-4} mm/year) by coating it with ULPEtA30, ULPEtA35, ULPEtA40 and ULPEtA45 nanocomposites. Moreover, an increase in polarization resistance was also observed.

The potentiodynamic polarizations for uncoated MS and ULPEtA nanocomposites coated MS after 175 h, and immersion in 5 wt% NaCl solution are given in Figure 9, and show that there was a remarkable potential shift to noble values for mild steel coated with ULPEtA nanocomposites as compared to uncoated mild steel after immersion in 5 wt% NaCl. The various polarization parameters such as E_{corr} and I_{corr} obtained from cathodic and anodic

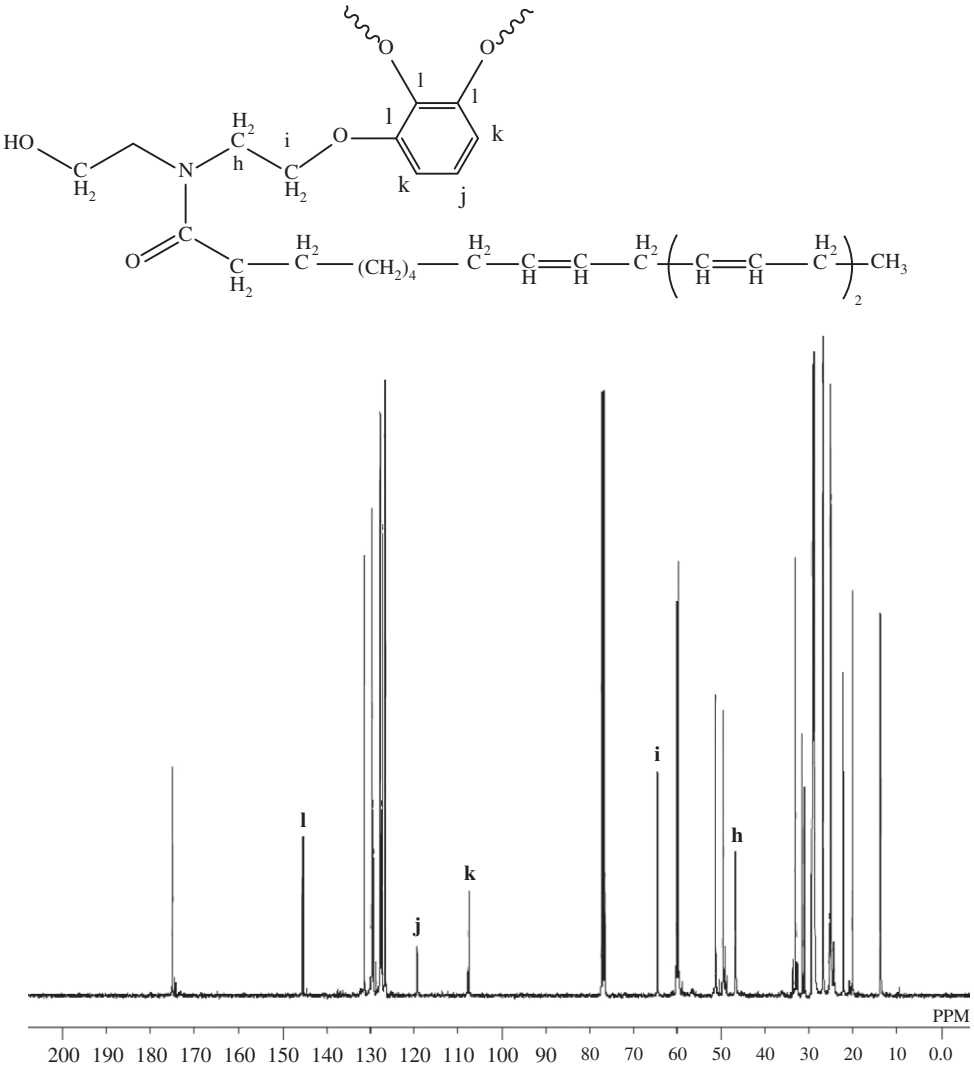

Figure 5: Carbon nuclear magnetic resonance (^{13}C-NMR) spectra of linseed polyetheramide (LPEtA).

curves are shown in Table 2, and indicate that E_{corr} and corrosion rate values for uncoated mild steel were obtained as 833.92 mV, 3.0539 mm/year. Corrosion rate can be controlled (6.4124×10^{-2} mm/year) by coating mild steel with ULPEtA30, ULPEtA35, ULPEtA40 and ULPEtA45 nanocomposites. The investigation clearly showed that ULPEtA nanocomposites coated on mild steel controlled both anodic and cathodic reactions and acted as a barrier. In the case of mild steel coated with ULPEtA30, ULPEtA35, ULPEtA40 and ULPEtA45 nanocomposites, E_{corr} values (Table 2) were found to increase with increase in the amount of IPDI in poly(urethane-etheramide). These coatings conferred barrier properties to the mild steel panel. The intact organic groups dispersed throughout the coatings, apparently serving to increase the hydrophobicity of coatings, repelling water, corrosion ions and enhancing corrosion protection properties, arising due to the cross linked network structure of ULPEtA nanocomposites.

The polarization curve recorded for uncoated MS and coated with ULPEtA nanocomposites after 250 h immersion in tap water is described in Figure 10. The cathodic and anodic polarization curves for Tafel regions were extrapolated and analyzed. E_{corr} and corrosion rate values for uncoated MS were found to be -583.60 mV and 7.6758×10^{-1} mm/year. The corrosion rate was controlled to lower values (2.778×10^{-6} mm/year) by coating it with ULPEtA nanocomposites.

The polarization curve recorded for uncoated MS and coated with ULPEtA nanocomposites after 2 h immersion in 3.5% NaOH is explained in Figure 11. The E_{corr} values shown in Table 2 indicated that ULPEtA incorporated a good combination of ether, amide, urethane and Fe_2O_3 nanoparticles, which provided strong adhesion to the

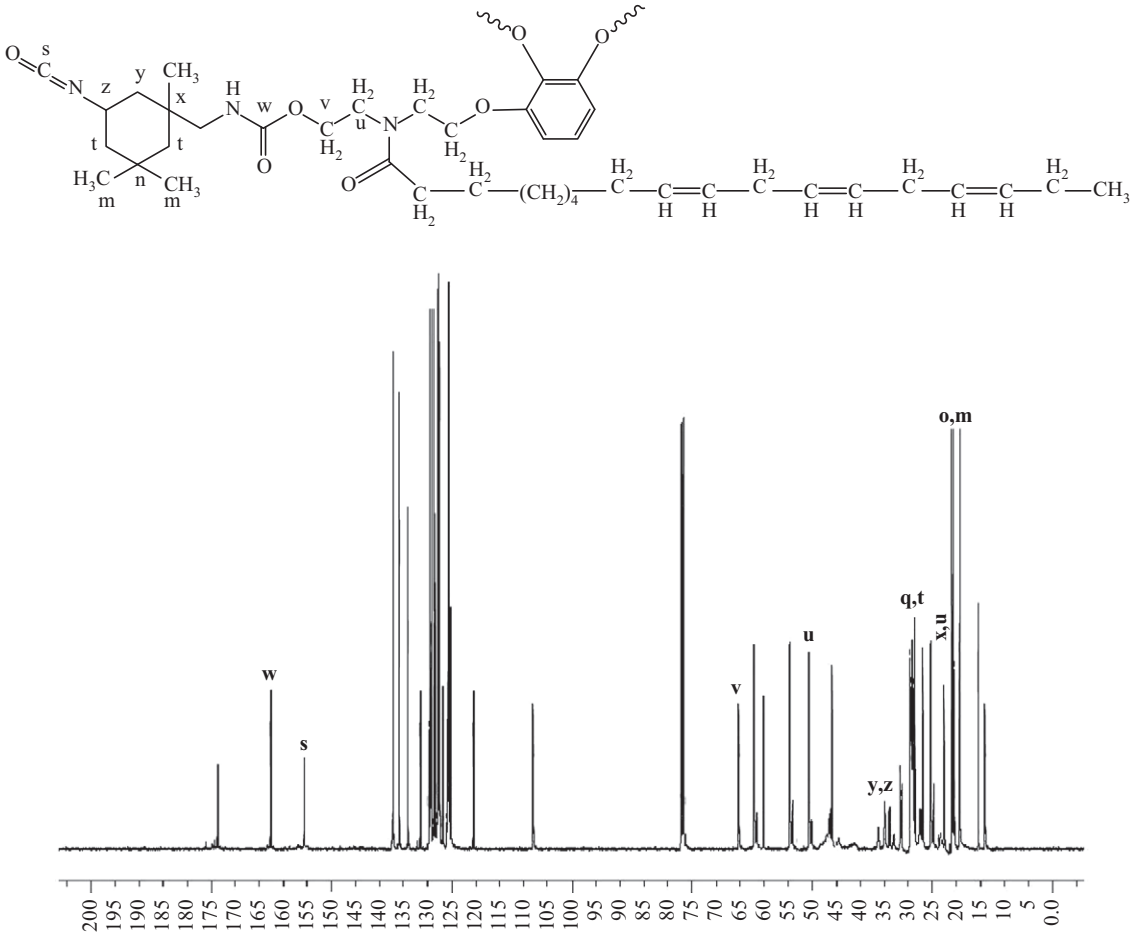

Figure 6: Carbon nuclear magnetic resonance (^{13}C-NMR) spectra of linseed poly(urethane-etheramide) (ULPEtA).

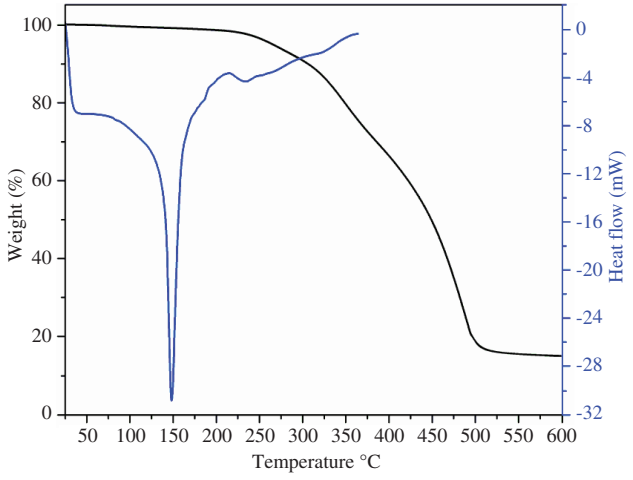

Figure 7: Differential scanning calorimetry (DSC)/thermogravimetric analysis (TGA) thermograms.

substrate. ULPEtA/Fe_2O_3 nanocomposite coatings displayed good resistance against acid, alkali and saline environment. The physico-mechanical performance revealed that ULPEtA40 showed the best performance amongst all compositions in different corrosive media.

3.7 SEM and EDX

The SEM micrograph (Figure 12) of ULPEtA/Fe_2O_3 nanocomposite coating showed a uniform surface, without any visible cracks and uniform dispersion of nanoparticles in the polymer matrix, which are not well-defined in shape. The EDX spectrum also supported that Fe_2O_3 nanoparticles were present in polymeric matrix.

EDX results (Figure 13) confirmed that Fe_2O_3 nanoparticles are dispersed in ULPEtA coating. The peaks observed at 0.3 keV, 0.4 keV and 0.6 keV correspond to the binding energies of C, N and O, respectively; peaks observed at 0.7 keV, 6.5 keV and 7.1 keV belong to Fe Lα, Fe Kα and Fe Kβ, respectively. These optical absorption peaks are typical of metallic iron nanocrystalline due to surface plasmon resonance.

Table 1: Physicochemical and physico-mechanical characterization of resins.

Resin code[a]	HELA	LPEA	ULPEtA30	ULPEtA35	ULPEtA40	ULPEtA45
Acid value	2.3	–	–	–	–	–
Hydroxyl value (%)	9.1	6.3	5.7	4.5	3.9	3.3
Iodine value	89	59	27.7	24.2	19.2	17.3
Refractive index	1.489	1.503	1.520	1.522	1.530	1.535
Impact resistance (lb/inch)			150	150	150	150
Gloss at 45°			94.1	93.2	97.3	97.9
Thickness (μm)	–	–	152	163	159	157
Pencil hardness	–	–	2B	4H	6H	4H
Scratch hardness (kg)	–	–	1.5	1.7	2.0	1.5
Bend test (1/8 inch)	–	–	Passes	Passes	Passes	Passes

[a]Last numeral digit indicates the% of isophorone diisocyanate (IPDI) in linseed polyetheramide (LPEtA).
HELA, N-N-bis (2-hydroxyethyl) linseed oil fatty amide; LPEA, linseed oil polyetheramide; ULPEtA, linseed poly(urethane-etheramide).

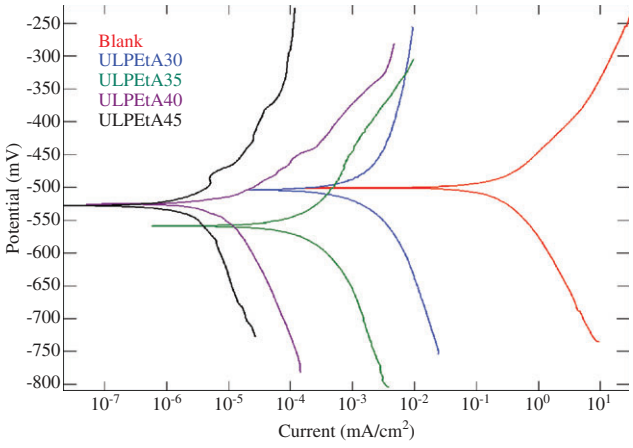

Figure 8: Tafel plots in 3.5 wt% HCl solution.

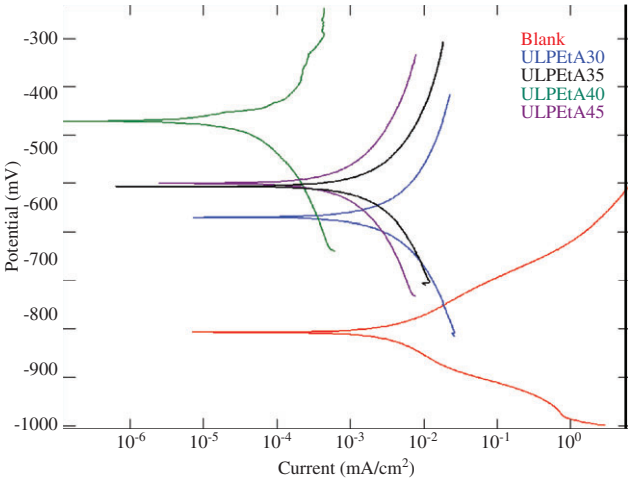

Figure 9: Tafel plots in 5 wt% NaCl solution.

Table 2: Corrosion parameter for coated and uncoated mild steel (MS) in different corrosive environments.

Sample code	Medium	E_{corr} (mV)	I_{corr} (mA/cm²)	Corrosion rate (mm/year)	Inhibition efficiency (%)
Mild steel	3.5 wt% HCl	-549.46	1.9208	22.262	–
ULPEtA30	3.5 wt% HCl	-504.50	5.3539×10^{-3}	6.20512×10^{-2}	99.72
ULPEtA35	3.5 wt% HCl	-554.35	1.1351×10^{-3}	1.31556×10^{-2}	99.94
ULPEtA40	3.5 wt% HCl	-531.24	5.843×10^{-4}	6.7726×10^{-3}	99.96
ULPEtA45	3.5 wt% HCl	-476.57	2.882×10^{-5}	3.341×10^{-4}	99.99
Mild steel	5.0 wt% NaCl	-833.92	0.26349	3.0539	–
ULPEtA30	5.0 wt% NaCl	-574.62	8.857×10^{-3}	1.02652×10^{-1}	96.63
ULPEtA35	5.0 wt% NaCl	-510.20	2.3768×10^{-3}	2.7547×10^{-2}	99.09
ULPEtA40	5.0 wt% NaCl	-378.08	1.243×10^{-4}	1.441×10^{-3}	99.95
ULPEtA45	5.0 wt% NaCl	-561.40	5.5327×10^{-3}	6.4124×10^{-2}	97.90
Mild steel	3.5 wt% NaOH	-418.47	1.0797×10^{-4}	1.25132×10^{-2}	–
ULPEtA30	3.5 wt% NaOH	-981.01	3.259×10^{-5}	3.777×10^{-4}	69.81
ULPEtA35	3.5 wt% NaOH	-572.10	4.077×10^{-6}	2.40726×10^{-2}	96.22
ULPEtA40	3.5 wt% NaOH	-657.17	6.615×10^{-7}	7.899×10^{-5}	99.39
ULPEtA45	3.5 wt% NaOH	-120.25	6.773×10^{-7}	7.85×10^{-6}	99.37
Mild steel	Tap water	-583.60	6.62278×10^{-2}	7.6758×10^{-1}	–
ULPEtA30	Tap water	-528.77	2.585×10^{-4}	2.9961×10^{-3}	99.60
ULPEtA35	Tap water	-484.50	7.778×10^{-5}	9.014×10^{-4}	99.88
ULPEtA40	Tap water	-52.896	5.133×10^{-7}	5.95×10^{-6}	99.99
ULPEtA45	Tap water	-80.313	2.397×10^{-7}	2.778×10^{-6}	99.99

ULPEtA, linseed poly(urethane-etheramide).

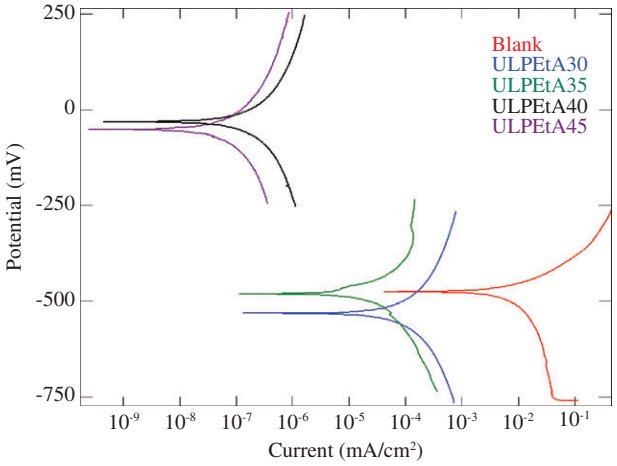

Figure 10: Tafel plots in tap water.

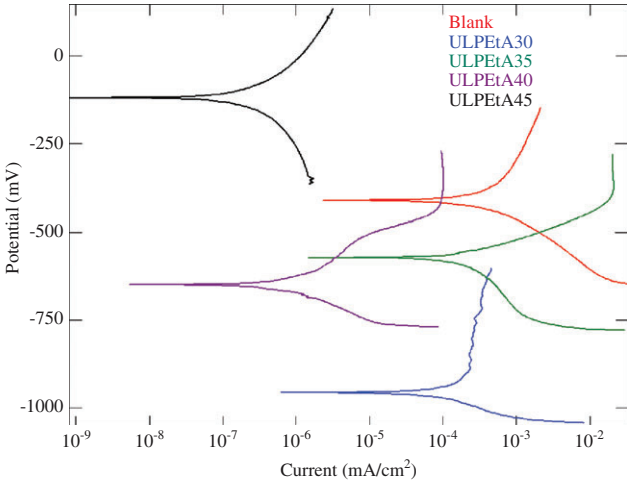

Figure 11: Tafel plots in 3.5 wt% NaOH solution.

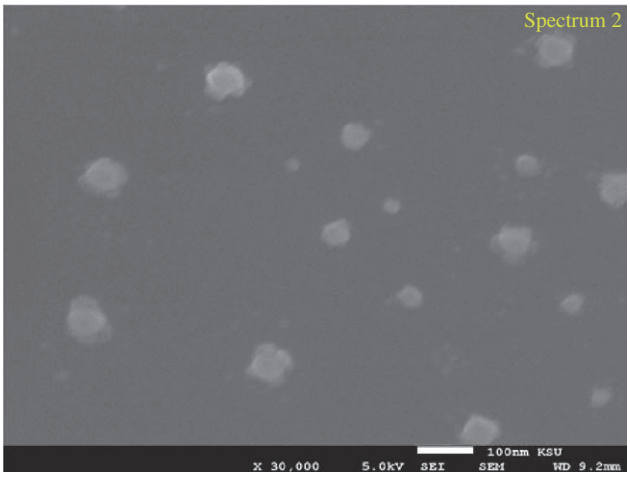

Figure 12: Scanning electron microscopy (SEM) of linseed poly(urethane-etheramide) (ULPEtA)/Fe_2O_3 nanocomposite.

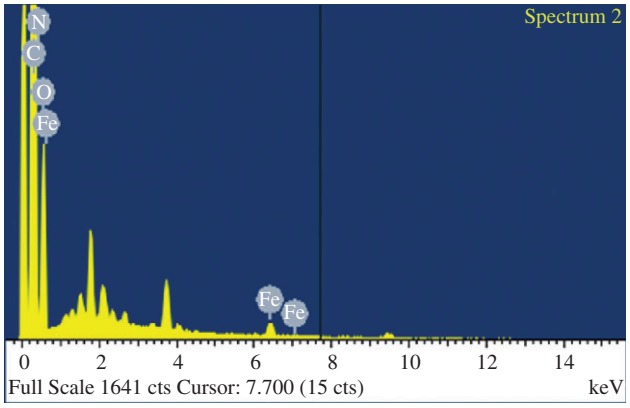

Figure 13: Energy dispersive X-ray (EDX) of linseed poly(urethane-etheramide) (ULPEtA)/Fe_2O_3 nanocomposite.

4 Conclusions

Linseed oil based urethane modified polyetheramide nanocomposite coatings were cured at room temperature. A novel combination of properties of amide, ether and urethane was present in the synthesized resins. ULPEtA40 nanocomposite coatings showed good scratch hardness, flexibility, gloss and corrosion resistance. ULPEtA40 can be safely used up to 220°C as an eco-friendly coating material.

Acknowledgments: This project was supported by King Saud University, Deanship of Scientific Research, College of Science-Research Center.

References

[1] Miranda TJ. In *Surface Coatings*, 3rd ed., Chapman & Hall: London, 1993, Vol. 1, p. 9.
[2] Schweitzer PA. *Corrosion-Resistant Linings and Coatings*, Marcel Dekker: New York, 2001, p. 301.
[3] Goldade VA, Pinchuk LS, Makarevich AV, Kestelman VN. *Plastics for Corrosion Inhibition*, Springer-Verlag: Berlin, 2005, Vol. 82, p. 175.
[4] Javni I, Petrovic ZS, Guo A, Fuller R. *J. Appl. Polym. Sci.* 2000, 77, 1723–1734.
[5] Aigbodion AI, Pillai CKS, Bakare IO, Yahaya LE. *Ind. J. Chem. Technol.* 2001, 8, 378–384.
[6] Alam M, Akram D, Sharmin E, Zafar F, Ahmad S. *Arabian J. Chem.* 2014, 7, 469–479.
[7] Meshram PD, Puri RG, Patil AL, Gite VV. *Prog. Org. Coat.* 2013, 76, 1144–1150.

[8] Can E, Kusefoglu S, Wool RP. *J. Appl. Polym. Sci.* 2002, 83, 972–980.
[9] Alam M, Alandis NM. *Ind. Crops Prod.* 2014, 57, 17–28.
[10] Lu Y, Larock RC. *ChemSusChem* 2009, 2, 136–147.
[11] Alam M, Ashraf SM, Ray AR, Ahmad S. *J. Polym Environ.* 2010, 18, 208–215.
[12] Alam M, Alandis NM. *High Perform. Polym.* 2012, 24, 538–545.
[13] Alam M, Alandis NM. *Prog. Org. Coat.* 2012, 75, 527–536.
[14] Alam M, Alandis NM. *Anti-Corros. Methods Mater.* 2014, 61, 232–240.
[15] Guo A, Cho Y, Petrovic ZS. *J. Polym. Sci. Part A: Polym. Chem.* 2000, 38, 3900–3910.
[16] Petrović ZS. *Polym. Rev.* 2008, 48, 109–155.
[17] Lligadas G, Ronda JC, Galia M, Cadiz V. *Biomacromolecules* 2010, 11, 2825–2835.
[18] Desroches M, Escouvois M, Auvergne R, Caillol S, Boutevin B. *Polym. Rev.* 2012, 52, 38–79.
[19] Pfister DP, Xia Y, Larock RC. *ChemSusChem* 2011, 4, 703–717.
[20] Siyanbola TO, Sasidhar K, Anjaneyulu B, Kumar KP, Rao BVSK, Narayan R, Olaofe O, Akintayo ET, Raju KVSN. *J. Mater. Sci.* 2013, 48, 8215–8227.
[21] Lligadas G, Ronda JC, Galia M, Cadiz V. *Biomacromolecules* 2006, 7, 2420–2426.
[22] Zlatanic A, Petrovic ZS, Dusek K. *Biomacromolecules* 2002, 3, 1048–1056.
[23] Rahman O, Ahmad S. *RSC Adv.* 2014, 4, 14936–14947.
[24] Dhoke SK, Khanna AS. *Corr. Sci.* 2009, 51, 6–20.
[25] Dhoke SK, Khanna AS. *Mater. Chem. Phys.* 2009, 117, 550–556.
[26] Rahman O, Kashid M, Ahmad S. *Prog. Org. Coat.* 2015, 80, 77–86.
[27] Alam M, Ray AR, Ashraf SM, Ahmad S. *J. Am. Oil Chem. Soc.* 2009, 6, 573–580.